

# Interpretation of the map of the universe

Deng Xiaoming

Chief Engineer Office, Kaiming Engineering Consultancy  
1607-1612, Huatian Building,  
6, North Xiaomachang, Haidian District, Beijing, PRC 100038

[dxmchina@yahoo.com.cn](mailto:dxmchina@yahoo.com.cn)

## Abstract

The redshift distribution of galaxies on the logarithmic map of the universe has been explained. Our computed result show that the density distribution of galaxies take two peaks at redshift 0.108 and 0.362 and two minimum at redshift 0.229 and 0.510. It is shown that our model may fit the map well. It is proposed that celestial sphere should be defined by the comoving coordinates system, and the SDSS data may bear out our supposition that the topology of our universe might be hypersphere.

**Key words:** redshift distribution, cosmic sound wave, large scale structure of the universe, redshift periodicity, SDSS, redshift survey, hyperspherical universe.

## 1. Introduction

J. Richard Gott III, et al. produced a new conformal map of the universe illustrating recent discoveries [1]. A magical logarithmic map of the universe shows us a panoramic view of the universe. The present paper will try to explain the section of the map run from redshift 0.01 to 4.196 by the linear expansion hyperspherical model.

Readers also may skip the following part in this section and start on section 2. As a matter of convenience for readers to follow the thread of our argument, first we review the useful equations, deductions or conclusions from before:

As we know, the R-W metric for the case of spherical space is

$$d\tau^2 = c^2 dt^2 - R^2(t)[d\alpha^2 + \sin^2\alpha(d\theta^2 + \sin^2\theta d\phi^2)]$$

If  $R(t)=kt$  [2][3](k is a constant), then

$$\int_t^{t_0} \frac{cdt}{R(t)} = \int_0^\alpha d\alpha, \quad \int_t^{t_0} \frac{cdt}{kt} = \int_0^\alpha d\alpha \quad \text{and} \quad \frac{k\alpha}{c} = \ln \frac{t_0}{t}.$$

For  $\frac{R(t_0)}{R(t)} = \frac{t_0}{t} = 1 + Z$ , we have the redshift formula

$$\frac{k\alpha}{c} = \ln(1 + Z) \tag{1}$$

We know that the period of Bolometric flux in the linear expansion hyperspherical universe is  $\pi$  [4][3]. If we consider that Karlsson's quasar redshift periodicity [5][6] (statistical formula  $\Delta \ln(1 + Z) \approx 0.206$ ) may be caused by the quasars nearby poles  $\alpha=\pi, 2\pi, 3\pi\dots$ (see the polar effect or the lens effect of cosmic entire space [2][3][4]), Eq. (1) can be written as:

$\ln(1+Z_n) = \frac{k\alpha_n}{c} = \frac{k(n\pi + \Delta\alpha)}{c}$ ,  $n=1, 2, 3, \dots$ , where  $\Delta\alpha$  is a infinitesimal. The period is:

$$\alpha_{n+1} - \alpha_n = \pi, \text{ then } \Delta\ln(1+Z) = \ln(1+Z_{n+1}) - \ln(1+Z_n) = \ln \frac{1+Z_{n+1}}{1+Z_n} = \frac{\pi k}{c}.$$

Let  $\Omega = \pi k/c$ , then  $\Delta\ln(1+Z) = \Omega$  and  $k = \Omega c/\pi$ . Where  $\Omega \sim 0.206$  is “the half periodic parameter”[2](as we had defined before). By the way, the significance of  $\Omega$  was first clearly understood in the paper titled the linear expansion hyperspherical universe [3]. By substituting  $k = \Omega c/\pi$  to Eq. (1), we have

$$\Omega\alpha/\pi = \ln(1+Z), \text{ or } Z = e^{\frac{\Omega\alpha}{\pi}} - 1. \tag{2}$$

Thus we obtain the solvable functional relations between redshift  $Z$  and coordinate  $\alpha$ .

Bolometric flux in the linear expansion hyperspherical universe is

$$l = \frac{L}{4\pi R^2(t_0)(1+Z)^2 \sin^2 \alpha}. \text{ Substituting Eq. (2) to the left equation, we have}$$

$$l = \frac{L}{4\pi R^2(t_0)e^{2\Omega\alpha/\pi} \sin^2 \alpha}, \text{ let } \mu_0 = \frac{L}{4\pi R^2(t_0)}, \text{ we obtain}$$

$$l = \frac{\mu_0}{e^{2\Omega\alpha/\pi} \sin^2 \alpha}. \tag{3}$$

Where  $\mu_0$  is a constant [3].

The periodic attenuation of Bolometric flux at identical phase position is

$$\frac{l(n\pi + \alpha_f)}{l(\alpha_f)} = \frac{1}{e^{2\Omega n}}, \quad n=0, 1, 2, 3, \dots \tag{4}$$

Where  $\alpha_f$  is a fixed phase and  $0 < \alpha_f < \pi$ .

The derived function of Eq.(3) is

$$\frac{dl}{d\alpha} = -\frac{2\mu_0}{e^{2\Omega\alpha/\pi} \sin^2 \alpha} \left( \frac{\Omega}{\pi} + ctg\alpha \right) \quad [3] \text{ and let } \frac{dl}{d\alpha} = 0, \text{ then } tg\alpha = -\frac{\pi}{\Omega}. \text{ Solving the equation, we obtain}$$

$$\alpha_n = n\pi + tg^{-1}\left(-\frac{\pi}{\Omega}\right), \quad n=1, 2, 3, \dots \tag{5}$$

Where  $\alpha_n$  is the positions where to get the interzone,  $\{n\pi, (n+1)\pi\}$   $n=0, 1, 2, \dots$ , minimum value of brightness  $l_{\min}$ .

In the present paper, we need the formula to show the number of galaxies distributed in the differential interval of  $\alpha$ . Since the derivation step is too long to be shown here, see paper [3], the formula is

$$\frac{dn}{d\alpha} = \frac{2N}{\pi} \sin^2 \alpha. \tag{6}$$

Where  $dn$  is the number of the galaxies in  $d\alpha$  and  $N$  is a constant, its signification is the total number of the galaxies in the universe.

## 2. Comoving coordinates and Celestial sphere

We have discussed about comoving coordinates system for the case of spherical space before [7],

and a figure is shown below

Reference Fig 1 (a), vector  $R$ ,  $R\sin\alpha$  and  $R\sin\alpha\sin\theta$  are on mutually perpendicular plane  $P_\alpha$ ,  $P_\theta$  and  $P_\phi$  respectively.

$$X_1=OA=R\sin\alpha\sin\theta\sin\phi; X_2=OB=R\sin\alpha\sin\theta\cos\phi; X_3=OC=R\sin\alpha\cos\theta; X_4=OD=R\cos\alpha$$

$$\text{We also have: } R^2=X_1^2+X_2^2+X_3^2+X_4^2=(OA)^2+(OB)^2+(OC)^2+(OD)^2$$

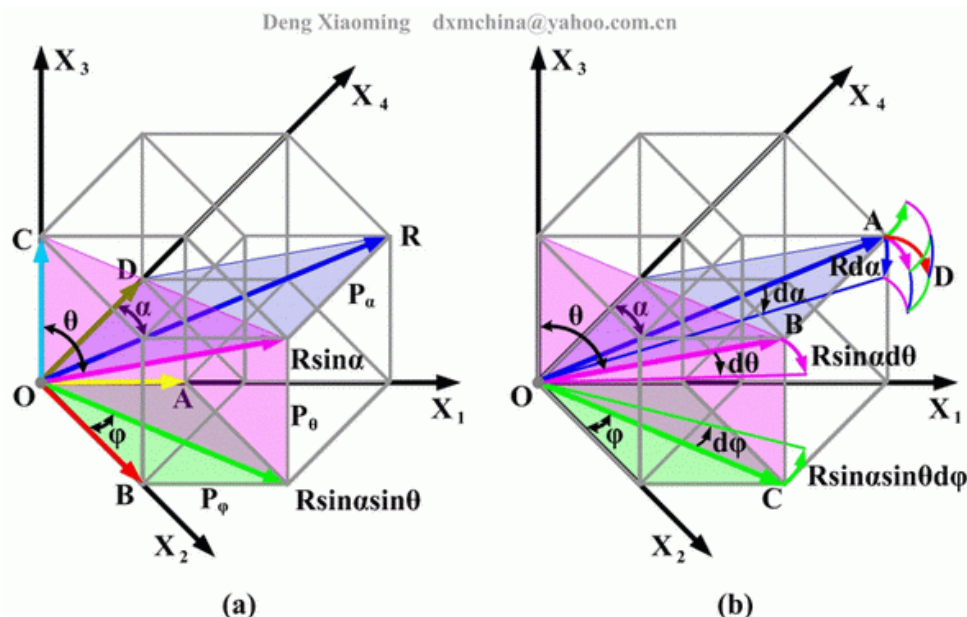


Figure 1 The hyperspherical coordinates in four-dimensional Euclidean space

Reference Fig 1 (b), on plane  $P_\alpha$ ,  $P_\theta$  and  $P_\phi$ , if angle increment of vector  $R$ ,  $R\sin\alpha$  and  $R\sin\alpha\sin\theta$  are  $d\alpha$ ,  $d\theta$  and  $d\phi$  respectively, the corresponding arc length are  $Rd\alpha$ ,  $R\sin\alpha d\theta$  and  $R\sin\alpha\sin\theta d\phi$ , then at the end of vector  $R$ , we have

$$AD^2=ds^2=(Rd\alpha)^2+(R\sin\alpha d\theta)^2+(R\sin\alpha\sin\theta d\phi)^2=R^2[d\alpha^2+\sin^2\alpha(d\theta^2+\sin^2\theta d\phi^2)]$$

The so-called comoving coordinates system should define celestial sphere in math. Before, we consider that the celestial sphere is an imaginary sphere of gigantic radius with the earth (or the sun) located at its center. Of course, such a coordinates system without altitude can not satisfy with modern astroobservation.

In fact, the celestial sphere system is not imaginary but really exists, they are uninterrupted cosmic historical section observed on earth. In cosmic three-dimensional curved space, there isn't any gigantic radius but the objective value of redshift (yes, we can give the radius  $r=R\sin\alpha$ , but nor significance here). It is the redshift that measure the spatial deepness between a celestial object and the earth. We have already set up the relation between redshift and comoving coordinates  $\alpha$  by Eq. (2).

See Fig 2 (a), in the linear expansion hyperspherical universe, the celestial sphere at  $\alpha=\pi/4$  (redshift 0.053);  $\pi/2$  (redshift 0.108);  $3\pi/4$  (redshift 0.167) are different in size and not concentric. Not like three-dimensional flat space, the size of the celestial sphere is maximum at  $\alpha=\pi/2$  (redshift 0.108) and zero at  $\alpha=0$  (redshift 0) and  $\pi$  (redshift 0.229). Because of cosmic expansion,

the celestial sphere at  $\alpha=\pi/4$  (redshift 0.053) is bigger than it at  $3\pi/4$  (redshift 0.167) in size. Where just is schematic, the same case is in normal region  $\{n\pi, (n+1)\pi\}$   $n=0, 1, 2, \dots$ . From the following discussion in next section, we will see that all galaxies with same redshifts are distributed on a certain celestial sphere.

For farther understanding, we might as well consider the two-dimensional case. See also Fig 2 (b), place our Earth at  $\alpha=0$  (the end of  $R_0$ ) on the sphere  $S_0$  (note that the different spheres  $S_n, n=0, 1, 2, \dots$  are the cosmic evanescence space). The loops at  $\alpha=\pi/4$  on the sphere  $S_1$ , at  $\alpha=\pi/2$  on the sphere  $S_2$  and at  $\alpha=3\pi/4$  on the sphere  $S_3$  can be looked as, see also Fig 2 (a), the celestial spheres at  $\alpha=\pi/4$  (redshift 0.053), at  $\alpha=\pi/2$  (redshift 0.108) and at  $\alpha=3\pi/4$  (redshift 0.167) in three-dimensional case.

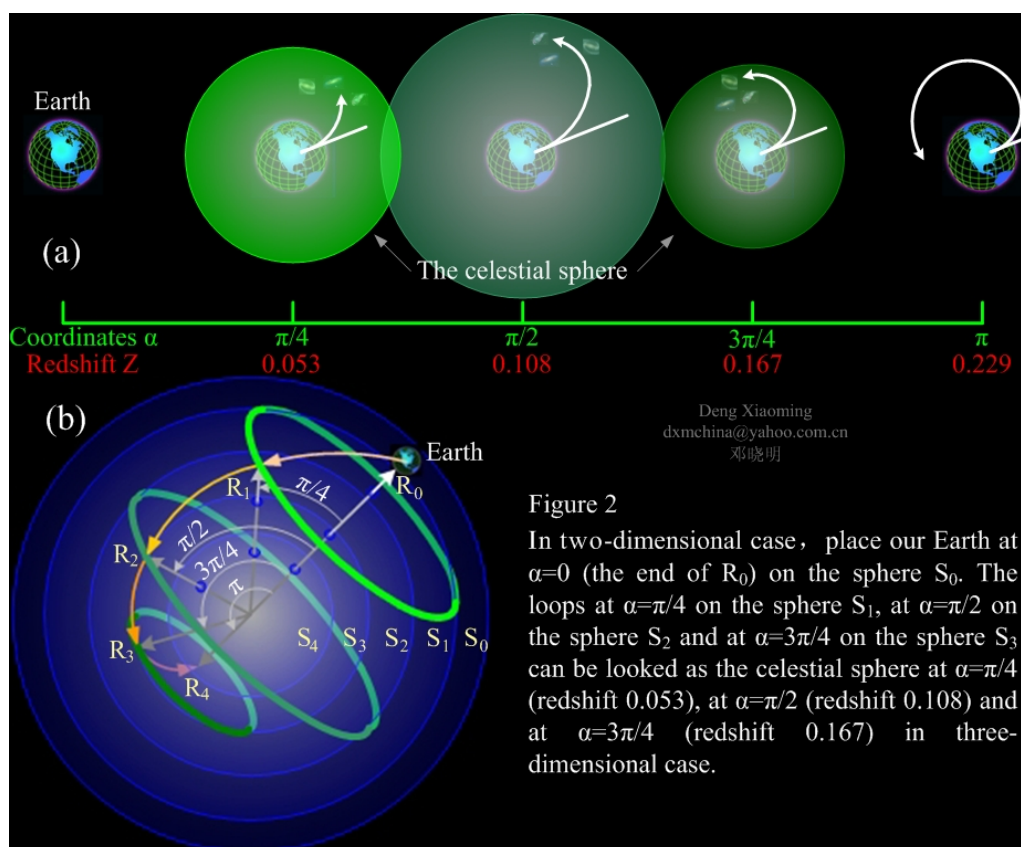


Figure 2  
In two-dimensional case, place our Earth at  $\alpha=0$  (the end of  $R_0$ ) on the sphere  $S_0$ . The loops at  $\alpha=\pi/4$  on the sphere  $S_1$ , at  $\alpha=\pi/2$  on the sphere  $S_2$  and at  $\alpha=3\pi/4$  on the sphere  $S_3$  can be looked as the celestial sphere at  $\alpha=\pi/4$  (redshift 0.053), at  $\alpha=\pi/2$  (redshift 0.108) and at  $\alpha=3\pi/4$  (redshift 0.167) in three-dimensional case.

### 3. To interpret the logarithmic map of the universe from redshift 0.01 to 4.196

J. Richard Gott III and his partners [1] have produced a new conformal map of the universe illustrating recent discoveries. On this, we are only interested in the region run from redshift 0.01 to 4.196. The dots appearing beyond M81 in their map are the 126,594 SDSS galaxies and quasars (with  $z < 5$ ) in the equatorial plane ( $-2^\circ < \delta < 2^\circ$ ), but these exclude regions 3.7hr~8.7hr, and approximately 16.7hr~20.7hr because they cover the zone of avoidance close to the Galactic plane. The selective space form is flat case, they project the slices directly onto a two-dimensional flat sheet.

Before farther discussion, we might as well notice that space types would affect the interpretation of a sample. See also Fig 2, if the cosmic space is hypersphere, the 3D picture or video that we used to demonstrate redshift slice survey would poses an optical illusion. Especially, the density distribution of galaxies would be factitiously diluted with the increase of redshift distance on the

fan-shaped cone diagram.

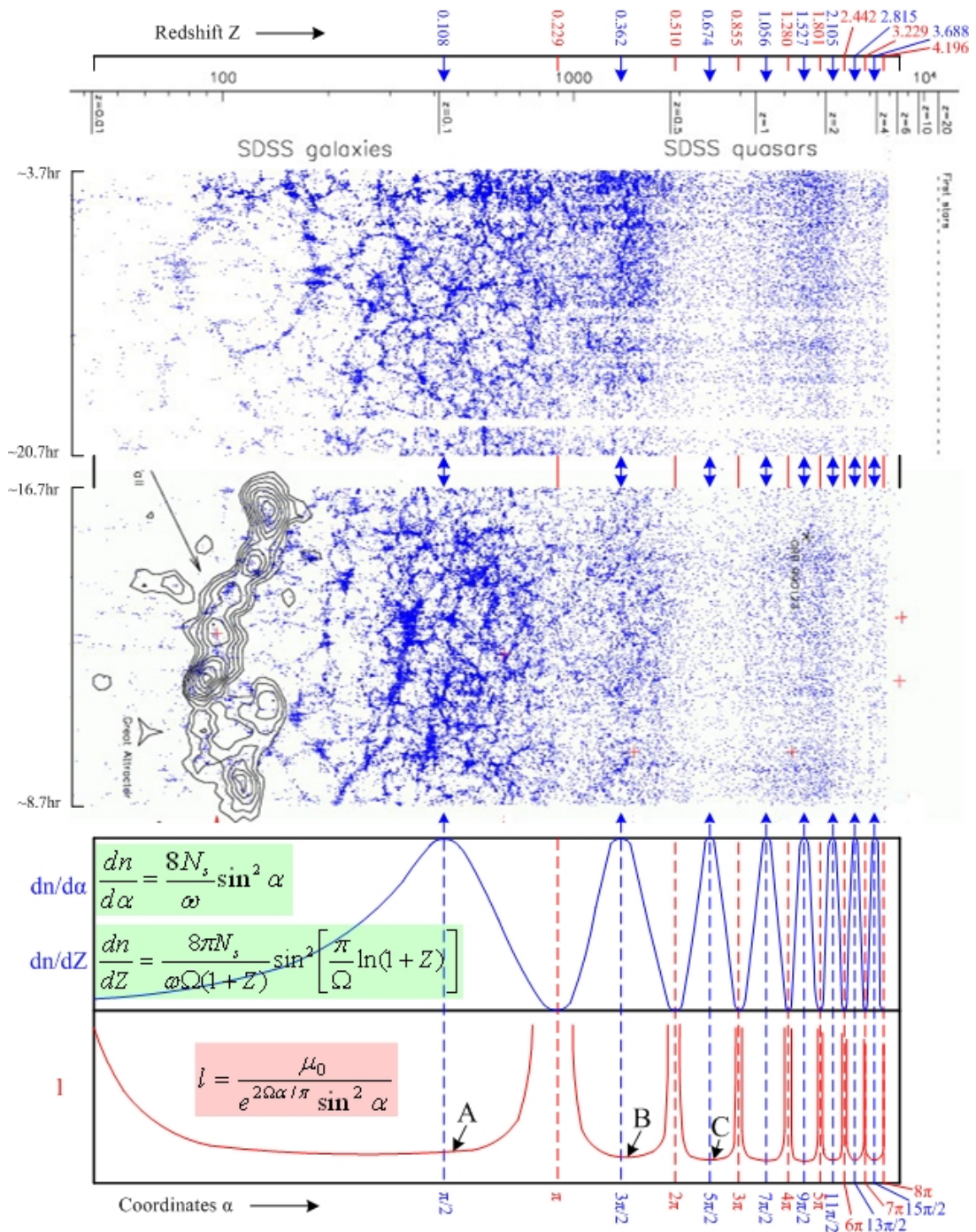


Figure 3 Above 8.7hr is the clipping of the logarithmic map of the universe

It is a great work indeed! When we got the first glance at the visual aid logarithmic map of the universe, what did we see? The rhythmic pattern of the universe came into view! It is such a projection that reveals the rhythmic features of the cosmic large-scale structure on two-dimensional rectangle plan. With the map that apparently accord with our visual habits, we can go in-depth step.

First, we put our mark symbol on the clippings of the map run from redshift 0.01 to the top, see Fig 3.

We have fully discussed about the distribution of galaxies and quasars in the linear expansion hyperspherical universe [3], and obtain the versiform Bolometric flux marked with Eq. (3) in this paper:

$$l = \frac{\mu_0}{e^{2\Omega\alpha/\pi} \sin^2 \alpha} \quad [3].$$

Where  $\Omega=0.206$ ;  $\mu_0=L/4\pi R^2(t_0)$  is a constant. L is the absolute luminosity of an emission sources located at coordinates  $\alpha$ , and l is its brightness observed by us at  $\alpha=0$  (or time  $t_0$ ). For the record, L also can be defined as  $L_{\text{galaxy}}$ ,  $L_{\text{star}}$  or  $L_{\text{other}}$  ...according to different subjects investigated.

The number of galaxies distributed in the differential interval of  $\alpha$  is Eq. (6):

$$\frac{dn}{d\alpha} = \frac{2N}{\pi} \sin^2 \alpha \quad [3].$$

Where dn is the number of the galaxies in  $d\alpha$  and N is a constant, its signification is the total number of the galaxies in the universe. Supposing that a survey covers a solid angle of  $\omega$  and  $N_s$  is the total number of galaxies in the solid angle, then  $N=4\pi N_s/\omega$ , and substituting it into above equation, we obtain another graspable form

$$\frac{dn}{d\alpha} = \frac{8N_s}{\omega} \sin^2 \alpha. \quad (7)$$

Where  $N_s/\omega$  is also constant.

By substituting Eq. (2) and its differential  $d\alpha = \frac{\pi}{\Omega(1+Z)} dZ$  to Eq. (7), we obtain other form

$$\frac{dn}{dZ} = \frac{8\pi N_s}{\omega \Omega(1+Z)} \sin^2 \left[ \frac{\pi}{\Omega} \ln(1+Z) \right]. \quad (8)$$

See also Fig 3, the distribution graph of  $dn/d\alpha$  or  $dn/dZ$  take two peak values at redshift 0.108 ( $\alpha=\pi/2$ ) and 0.362 ( $\alpha=3\pi/2$ ), and take two minimum values at redshift 0.229 ( $\alpha=\pi$ ) and 0.510 ( $\alpha=2\pi$ ) in the region redshift  $Z<0.510$  or  $\alpha<2\pi$ . Our model seems to fit the map well.

We are only interested in the positions where the peak values and minimum values obtained, and do not care too much about the distribution form because there are several influence factors to distort the distribution curve. Such as the foreground celestial objects is hiding the background celestial objects from view; brightness variation of distant celestial objects; the distortion in size [4] etc. All of these factors result in missing galaxies in some part or making up the number in other part in sample space. Hereon we just discuss about the case of distortion in brightness.

See also Fig 3, the bottom curve shows that the brightness of celestial objects nearby poles [3]( $\alpha=n\pi$ ,  $n=1, 2, 3...$  or redshift 0.229, 0.510, 0.855...) is brighter than they at other parts. The brightness of celestial objects marked as A, B, C...at  $\alpha=\alpha_n$ , see Eq. (5), get the interzone minimum value, and the concrete value of Eq. (5) is  $\alpha_n=n\pi-1.50532$ . It is seen that  $\alpha_n$  is nearby  $n\pi-\pi/2$ ,  $n=1, 2, 3....$

Comparing the brightness curve with the distribution graph of  $dn/d\alpha$  or  $dn/dZ$  in Fig 3, we see that the number of galaxies on the celestial sphere at  $\alpha=\pi/2$  and  $3\pi/2$  or redshift distance 0.108 and 0.362 get maximum value, see both Fig 2 and 3, but the brightness of the galaxies nearby the two points are the minimum value. It means that there are more missed galaxies around the two

regions. In contrast, the number of galaxies on the celestial sphere nearby  $\alpha=\pi$  and  $2\pi$  or redshift distance 0.229 and 0.510 is close to zero, but the brightness of the galaxies nearby the two points is at maximum. This means that there is less or no missed galaxies around the two regions, and even some dark or dwarf galaxies appear to be there to make up the number.

Fig 3 shows that our fundamental concern is the region run from the redshift 0.01 to 0.510 ( $\alpha<2\pi$ ), where most of the celestial objects are SDSS galaxies. Especially, the “fingerprint” of our universe is vivid in the region run from the redshift 0.01 to 0.229 ( $\alpha<\pi$ ), and thereinto contains all famous patterns, such as the great wall etc. In the region  $\alpha=\pi$  to  $2\pi$  or the redshift 0.229 to 0.510, It looks a bit faint but the ridge along redshift 0.362 in vertical direction is obvious, and the valley along the redshift 0.510 in vertical direction is still visible.

See Eq. (4), there is the periodic attenuation of Bolometric flux, and the degree of attenuation at

identical phase position is  $\frac{l(n\pi + \alpha_f)}{l(\alpha_f)} = \frac{1}{e^{2\Omega n}}$ ,  $n=0, 1, 2, 3\dots$ . Where  $\alpha_f$  is a fixed phase and

$0<\alpha_f<\pi$ . Supposing that the interzone  $\{n\pi, (n+1)\pi\}$   $n=0, 1, 2\dots$  lowest brightness in Fig 3 are  $l_A, l_B, l_C \dots$ (see points A, B and C), if  $l(\alpha_f)=l_A$ , according to the formula, then  $l_B=l_A/e^{2\Omega}$  and  $l_C=l_A/e^{4\Omega} \dots$ , since  $\Omega=0.206$ ,  $l_B$  is 66.2% of  $l_A$  and  $l_C$  is 43.9% of  $l_A$  through exponential decay.

Supposing that  $l_g$  (brightness) express the minimal Bolometric flux of galaxies that can be discerned by receiver. If  $l_A > l_g$  in Fig 3, it means that all of the galaxies in the region from redshift 0.01 to 0.229 or  $\alpha<\pi$  could be seen, and if  $l_A < l_g$ , some of galaxies would be missed. By the way, the value of  $l_g$  will become smaller and smaller with the development of the astronomical telescope.

See also Fig 3, in the region from redshift 0.229 to 0.510 or  $\alpha=\pi$  to  $2\pi$ ,  $l_B$  is 66.2% of  $l_A$ , considering the bottom of brightness curve is relatively flat, it means that more galaxies were missing. Furthermore, in the region from redshift 0.510 to 0.855 or  $\alpha=2\pi$  to  $3\pi$ ,  $l_C$  is 43.9% of  $l_A$ , which means that we could hardly see galaxies except those that are not too far from the poles ( $\alpha=n\pi, n=1, 2, 3\dots$ ). Maybe this case corresponds to our guess. In fact, there should be more galaxies around the redshift 0.674 or  $\alpha=5\pi/2$ , but they are too dark to be seen. It is seen that geometrical factor predominate if and how many galaxies can be seen in the region redshift  $Z<0.510$  or  $\alpha<2\pi$ , but beyond the region, the flux would be the leading factor.

On the map, beyond the redshift 0.510 (or  $\alpha > 2\pi$ ), most of the celestial objects are SDSS quasars. As we know, the condition of quasars is completely different from galaxies. See also Eq. (3) and  $\mu_0=L/4\pi R^2(t_0)$ , as a matter of distinction, the absolute luminosity  $L$  of celestial objects also can be defined as  $L_{\text{galaxy}}$  of galaxy,  $L_{\text{star}}$  of star and  $L_{\text{other}}$  of other celestial objects (such as active galactic nucleus)...according to different subjects investigated. The absolute luminosity of galaxy has been discussed before [3].  $L_{\text{galaxy}}$  may be regarded as the average of absolute luminosities of all galaxies (except for so called dwarf galaxy), and the evolution effect can be negligible, so we have reason to consider  $L_{\text{galaxy}}$  as a constant since galaxy formation. The condition of quasars is a problem of such perplexity. First, we don't definitely know what quasar is. We have loosely defined the quasar as the early star nearby the poles ( $\alpha=n\pi, n=1, 2, 3\dots$ )[3], but we cannot exclude the possibility that it is an active galactic nucleus which is a bit far from the poles or some material form on the course of evolution of galaxies etc. Maybe, all of them can be defined as different types of quasars. If the case is so, a serious consequence is that  $L_{\text{other}}$  is in uncertainty. Without the invariant  $L_{\text{other}}$ , we can't research on this issue. Fortunately, according to the linear expansion hyperspherical model [2][3][4], this type of quasar defined as the early star nearby the poles must exists, and its absolute luminosity is  $L_{\text{star}}$  of star. It is precise because there is this type of quasar that the quasar redshift periodicity was found [5][6].

Beyond the redshift 0.855 (or  $\alpha > 3\pi$ ), because the poles  $4\pi, 5\pi, 6\pi, 7\pi$  and  $8\pi$  are crowd together excessively, it is hard to tell apart. In order to study distant quasars, a more complete sample is needed, and then we should screen out the different types of quasars.

#### 4. Redshift distribution

The clippings of logarithmic map of the universe [1] show us the great ripples on plane. Although the form of distribution curve is distorted by several influence factors as we discussed above, we might as well give a simple analytic approximation to the redshift distribution on elevational drawing. See Fig 4, the redshift distribution of 2dFGRS radio sources (and all galaxies) (Colless 2001). The base map is from website: <http://www.roe.ac.uk/japwww/pust/cargese03/sld021.htm> or <http://www.aao.gov.au/htdocs/AAO/local/www/6df/Workshop2002/WWWtalks/sadler/sld007.htm>.

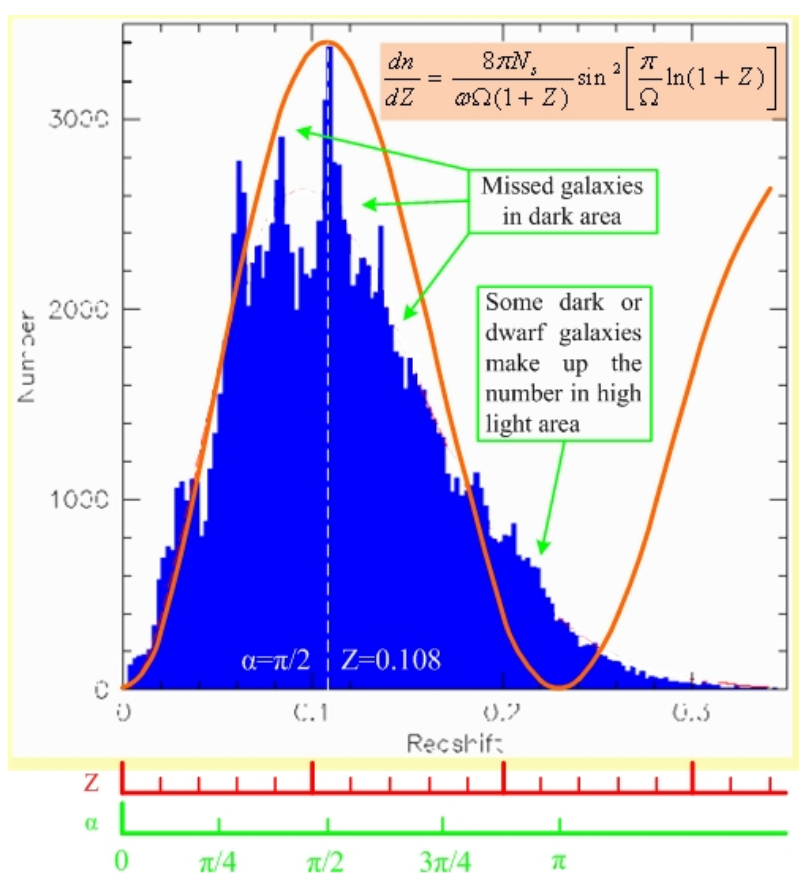


Figure 4 the redshift distribution of 2dFGRS radio sources (and all galaxies) base map from Colless 2001.

As we discussed above, It is seen that around redshift 0.108 or  $\alpha=\pi/2$ , there should be more galaxies in the data, but some galaxies must be missed because over there is dark area. In contrast, around the pole  $\alpha=\pi$  or redshift 0.229, there should be less galaxies in the data, but in the highlighted area, some dark or dwarf galaxies must make up the number. Because of 2dFGRS reached a depth of redshift  $Z\sim 0.3$ , beyond redshift 0.229 or  $\alpha=\pi$ , the data may be incomplete. In anyway, the position of the peak is accurate at redshift 0.108 or  $\alpha=\pi/2$ !

We have looked for the base map of SDSS on web, although it is not complete and so much as its irrelevancy for our case, we just want to give a schematic example. See Fig 5, the base map from

web site: <http://yummy.uchicago.edu/SDSS/>.

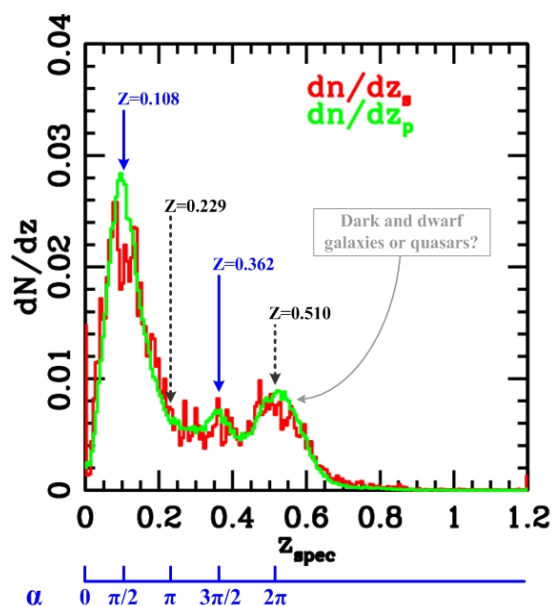


Figure 5 The redshift distribution of SDSS.  
The base map from Carlos Cunha, et al.

It is seen that two peaks at redshift 0.108 and 0.362 is fitted with our computed result, and the valley (pole  $\pi$ ) at redshift 0.229 is a little off the point because of the effect of high light. Around pole  $2\pi$  or redshift 0.510, same as pole  $\pi$ , it is affected by high light, we guess that most of objects over there would be dark and dwarf galaxies or quasars.

## 5. Conclusion

After we explained why “the great wall” is at redshift  $Z=0.079$  in fan-shaped redshift space [3], in the present paper, we might have unscrambled the logarithmic map of the universe [1] run from redshift 0.01 to 4.196 by our cosmic model [2][3][4], and it is seen that the computational result is fitting the map in the region run from the redshift 0.01 to 0.674 or  $\alpha < 5\pi/2$ . Especially, the computational result also show that the distribution of galaxies take two peak values at redshift 0.108 ( $\alpha=\pi/2$ ) and 0.362 ( $\alpha=3\pi/2$ ), and take two minimum values at redshift 0.229 ( $\alpha=\pi$ ) and 0.510 ( $\alpha=2\pi$ ) in the region redshift  $Z \leq 0.510$  or  $\alpha \leq 2\pi$ .

According to the above discussion, it is reconfirmed that the topology of our universe might be the linear expansion hypersphere.

## Acknowledgment

My grateful thanks to Professor He Xiangtao for his solicitude and edification and thanks to my daughter Amanda Deng in USA for her checking and annotating in language.

## References

- [1] J. Richard Gott III, et al. a Map of the Universe. The Astrophysical Journal, 624: 463-484, May 10, 2005.
- [2] Deng Xiaoming. The geometric characteristics of the universe.

- <http://www.paper.edu.cn>. October 31, 2005.
- [3] Deng Xiaoming. The linear expansion hyperspherical universe. <http://www.paper.edu.cn>.  
March 7, 2006.
- [4] Deng Xiaoming. The lens effect of cosmic entire hyperspherical space.  
<http://www.paper.edu.cn>. December 27, 2005.
- [5] Karlsson, K. G. Possible discretization of quasar redshifts. *Astron. Astrophys.* 13. 333, 1971.
- [6] Karlsson, K. G. On the existence of significant peaks in the quasar redshift distribution.  
*Astron. Astrophys.* 58, 237, 1977.
- [7] Deng Xiaoming. Graphic solution of R-W metric for the case of positive curvature and  
cosmic entire space and time. <http://www.paper.edu.cn>. January 20, 2006.